TABLE I

δ_K VALUES FROM CYCLOALKYL RADICALS AND CALCULATED IONIZATION POTENTIALS OF CORRESPONDING CYCLIC AMINES

Radical	δ_K(ev.)	Cyclic amine	I (amine, calcd., ev.)
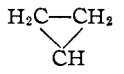	1.91	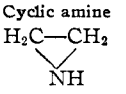	8.24
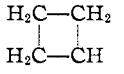	2.08	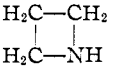	8.07
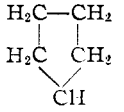	2.17	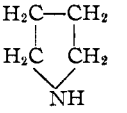	7.98
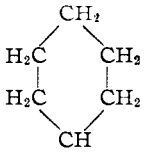	2.30	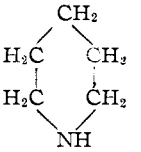	7.85

(R_2) — 0.05 ev. Apparently the non-planarity of the cycloalkyl radicals and ions has only a negligible effect on the overall behavior of ionization potential with substitution.

Since the equivalence of substituent groups on ionization potentials of radicals and corresponding amines has already been proven, it should now be possible to utilize δ_K values obtained from cycloalkyl radicals to calculate the ionization potentials of cyclic saturated amines. These are shown in Table I. The experimental values eventually to be compared with the calculated ionization potentials of the cyclic amines should come from photoionization or spectroscopic measurements since there is much scatter in the measured electron photoionization or spectroscopic measurements impact values.[4]

Ionization potentials of free radicals are of importance in appearance potential studies, in electronegativity considerations, in the determination of free radicals by gas chromatography using ionization detection and in many other applications. Ionization potentials of substituted amines are of interest in connection with the theory of charge-transfer complexes and in determining relative basicities unhampered by steric effects. It now appears that the calculation of ionization potentials by the use of δ_K values has a general validity even beyond that assumed in the original article and should enable one to estimate many values, necessary for experimental planning and theoretical interpretation, that have not yet been measured experimentally.

Acknowledgment.—The author should like to thank Dr. F. P. Lossing for graciously sending information on experimentally measured ionization potentials in advance of publication.

(4) R. W. Kiser, "Tables of Ionization Potentials," TID-6142 U.S. A.E.C., June 20, 1960.

[CONTRIBUTION FROM THE DEPARTMENT OF CHEMISTRY, UNIVERSITY OF CALIFORNIA, BERKELEY 4, CALIFORNIA]

Photochemical Oxidations. I. Ethyl Iodide

BY JULIAN HEICKLEN AND HAROLD S. JOHNSTON

RECEIVED JULY 9, 1962

The room temperature (25 ± 2°) photo-oxidation of ethyl iodide (0.06 to 2.8 mm.) in oxygen (2.8 mm.) with continuous ultraviolet radiation (usually above 2200 Å.) has been studied by irradiation in a cylindrical volume with a pinhole leak directly into a Bendix model 14 time-of-flight mass spectrometer. The initial products observed are C_2H_5OH, CH_3CHO, and I_2 in large amounts and $C_2H_5OOC_2H_5$, C_2H_5OOH, and C_2H_5OI in small amounts. Because of the cracking pattern of the reactants, it was impossible to establish the presence or absence of CH_4, C_2H_2, C_2H_4, C_2H_6, $HCHO_2$, CO_2 and HI. From mass balance HI was inferred to be a minor initial product. A fairly satisfactory nine-step mechanism can be found for the initial rate data, and several ratios of rate constants were evaluated from the data. The reaction was studied to about three per cent. completion, at which point diffusion of products through the pin-hole balanced the rate of photochemical production. The rate of attainment of this steady state and the steady-state pressures gave additional information beyond that found for the initial rates. The reaction at a few per cent. conversion of ethyl iodide is much more complex than the initial reaction: there is secondary production of alcohol, strong secondary destruction (perhaps largely heterogeneous) of C_2H_5OOH and C_2H_5OI, and slight over-all inhibition by I_2. Water was observed as a secondary product, coming in after a pronounced induction period. Even with a 14-step mechanism, all features of the reaction at three per cent. completion could not be explained. Although considerable effort was directed toward finding ozone in this system, it was never present in an amount as great as 10^{-8} atm.

Introduction

The photo-oxidation of methyl iodide has been studied extensively.[1-4] In recent years there has been agreement that the primary photochemical act is dissociation of the iodide

$$RI + h\nu \longrightarrow R + I \qquad (a)$$

in the presence of oxygen the radical forms the peroxy radical, iodine atoms associate to form molecular iodine, and the molecular iodine formed provides competition[4] with the oxygen for the alkyl radical

$$R + O_2 + M \longrightarrow RO_2 + M \qquad (b)$$

$$I + I + M \longrightarrow I_2 + M \qquad (c)$$

$$R + I_2 \longrightarrow RI + I \qquad (d)$$

For methyl radicals Christie[4] found the ratio of rate constants, k_b/k_d, to be 5.4×10^3 cc./mole and 5.4×10^2 cc./mole when M is CH_3I and CO_2, respectively.

(1) J. R. Bates and R. Spence, *J. Am. Chem. Soc.*, **53**, 1689 (1931); J. R. Bates and R. Spence, *Trans. Faraday Soc.*, **27**, 468 (1931).

(2) W. J. Blaedel, R. A. Ogg, Jr., and P. A. Leighton, *J. Am. Chem. Soc.*, **64**, 2500 (1942).

(3) R. B. Martin and W. A. Noyes, Jr., *ibid.*, **75**, 4183 (1953).

(4) M. I. Christie, *Proc. Roy. Soc.* (*London*), **A244**, 411 (1958).

The oxidation of methyl and ethyl radicals at room temperature has been studied by the mercury-photosensitized oxidation of methane and ethane,[5-7] in the radiolysis of mixtures of methane and oxygen,[8] in the photo-oxidation of azomethane,[9-16] photo-oxidation of azoethane[17] and diethyl ketone.[18] The oxidation of isopropyl radicals has been studied in the photo-oxidation of isopropyl iodide and diisopropyl peroxide.[19] The extensive literature on combustion and related studies suggest some of the elementary steps that may occur in these systems.[20,21] The references cited do not give unanimous agreement. However it has been firmly established that the ROO radical does not abstract hydrogen atoms from stable molecules in the gas phase at room temperatures. In those systems in which HOO radical is present, it was suggested[7] that the hydroperoxide was formed by

$$ROO + HOO \longrightarrow ROOH + O_2$$

This step has since been confirmed by Bell and McDowell[22] when R is isobutyl. The hydroperoxide has not been reported for any system not containing HOO radicals except the azomethane-oxygen system (even here HOO may be present, as our results on methyl iodide photo-oxidation seem to indicate).

The more usual reaction of the peralkoxy radical is the bimolecular splitting out of a molecule of oxygen[20]

$$2ROO \longrightarrow 2RO + O_2 \qquad (e)$$

Repeatedly it has been proposed that the peroxy radical attacks oxygen to give ozone.[23-26,15]

$$ROO + O_2 \longrightarrow RO + O_3 \qquad (e')$$

These experiments were designed to test this latter process for peroxy-ethyl radicals. It is generally agreed that the major products of radical oxidation arise from the dismutation of oxy-alkyl radicals.

$$2C_2H_5O \longrightarrow C_2H_5OH + CH_3CHO \qquad (f)$$

Thus some process, either e, e′, or some other, must reduce ROO to RO rapidly. These radicals should also recombine to give the peroxides

$$2C_2H_5O \longrightarrow (C_2H_5O)_2 \qquad (g)$$

The choice of ethyl radicals for the first intensive study was determined by the desire to choose between steps e and e′. Methyl radicals in the presence of oxygen are known to produce some methyl hydroperoxide, CH_3OOH, whose mass is 48, the same as ozone. The cracking pattern of ethyl iodide is clear around mass 48, so that ozone produced by step e′ should be easily observed.

Experimental

In the present system shown in Fig. 1 the reaction mixtures were photolyzed in a cell with a pin-hole leak to a Bendix Model 14 time-of-flight mass spectrometer. In this way product analyses were immediate, and the initially formed products of the reaction, as well as subsequent products could be detected.

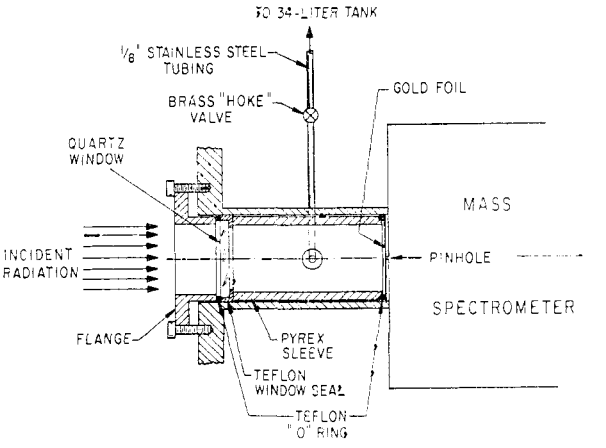

Fig. 1.—Schematic diagram of reaction cell, light source and mass spectrometer.

The cylindrically-shaped Pyrex reaction cell was 8.35 cm. long and 2.52 cm. in inside diameter. At one end was a 0.0038 cm. thick gold foil with a fine pin-hole leak 0.003 cm. in diameter which led directly to the electron gun of the mass spectrometer. At the other end was a quartz window through which the incident radiation passed. The cell was made vacuum tight with Teflon "o" rings. The entire reaction vessel rested in a stainless steel chamber with a 3-mm. stainless steel lead which connected the chamber to the vacuum line through a brass Hoke valve. The reaction mixtures were stored in a 34-liter stainless steel tank and flowed continuously into the reaction vessel through an opening in the side of the Pyrex sleeve. In this way the total pressure, which was measured continuously, was maintained nearly constant during a run. The total free volume including the 3-mm. stainless steel lead was 57.9 cc. up to the entrance valve. The volume inside the Pyrex sleeve, and thus the effective illuminated volume was 41.3 cc.

The reaction system and its leads were, unfortunately, quite heterogeneous, containing quartz, Pyrex, gold, Teflon, stainless steel, and brass. However, at the total pressures of the runs, between 1 and 20 mm., the time to diffuse one cm. is between 0.45×10^{-2} and 9.0×10^{-2} seconds. Thus species with lifetimes smaller than 10^{-2} seconds (*i.e.*, short-lived free radicals) will react before contacting a wall. Species with lifetimes of the order of 0.1 second (longer-lived free radicals) will have a good chance of reaching the wall before reacting. However, because of the Pyrex liner, these species will not contact stainless steel or brass. Also the possibility of their contacting teflon is small. Some experiments were done with a stainless steel liner and the

(5) J. A. Gray, *J. Chem. Soc.*, 3150 (1952).
(6) For a review see N. V. Fok and A. B. Nalbandyan, *Doklady Akad. Nauk S.S.S.R.*, 219 (1955). In particular see A. B. Nalbandyan, *Zhur. Fiz. Khim.*, **22**, 1443 (1948).
(7) J. S. Watson and B. deB. Darwent, *J. Phys. Chem.*, **61**, 577 (1957).
(8) G. Johnson and G. Salmon, *ibid.*, **65**, 177 (1961).
(9) G. R. Hoey and K. O. Kutschke, *Can. J. Chem.*, **33**, 496 (1955).
(10) R. L. Strong and K. O. Kutschke, *ibid.*, **37**, 1456 (1959).
(11) F. Wenger and K. O. Kutschke, *ibid.*, **37**, 1546 (1959).
(12) M. Shanin and K. O. Kutschke, *ibid.*, **39**, 73 (1961).
(13) M. Shanin and K. O. Kutschke, *J. Phys. Chem.*, **65**, 189 (1961).
(14) W. C. Sleppy and J. G. Calvert, *J. Am. Chem. Soc.*, **81**, 769 (1959).
(15) P. L. Hanst and J. G. Calvert, *J. Phys. Chem.*, **63**, 71 (1959).
(16) (a) N. R. Subbaratnam and J. G. Calvert, Stanford Research Institute International Symposium on Chemical Reactions in the Lower and Upper Atmosphere, April 18–20, 1961, *J. Am. Chem. Soc.*, **84**, 1113 (1962). (b) D. F. Dever and J. G. Calvert, *ibid.*, **84**, 1362 (1962).
(17) H. Cerfontain, "Photo-oxidation of Azoethane," Vitgeveri, Excelsior, Orangeplein 96, S. Gravenhage (1958).
(18) J. E. Jolley, *J. Am. Chem. Soc.*, **79**, 1537 (1957).
(19) G. R. McMillan, *J. Phys. Chem.*, **63**, 1526 (1959); *J. Am. Chem. Soc.*, **83**, 3018 (1961).
(20) J. H. Raley, L. M. Porter, F. F. Rust and W. E. Vaughan, *ibid.*, **73**, 15 (1951).
(21) "Oxidation," Discussion of the Faraday Society, London, 1945.
(22) K. M. Bell and C. A. McDowell, *Can. J. Chem.*, **39**, 1424 (1961).
(23) Ref. 21, p. 222.
(24) F. E. Blacet and R. P. Taylor, *Ind. Eng. Chem.*, **48**, 1505 (1956).
(25) C. C. Schubert and R. N. Pease, *J. Chem. Phys.*, **24**, 919 (1956).
(26) C. S. Schubert and R. N. Pease, *J. Am. Chem. Soc.*, **78**, 2044 (1956).

results were quantitatively different from those with a Pyrex liner. Species with longer lifetimes (*i.e.*, product molecules) will diffuse to fill the entire volume uniformly (the half-life of leakage through the gold-foil pinhole is about 240 seconds which is large compared to the internal diffusion times.)

The incident radiation was from a Hanovia type 528B 1000 watt Hg–Xe arc operating at 13.5 amperes and entered the reaction cell directly or through a neutral density screen and/or a Corning glass filter before entering the cell. The pressures of reactants were such that rarely was more than ten per cent. of the light absorbed. Thus the radical concentrations were uniform throughout the illuminated volume. However, in some of the experiments with the alkyl iodides the light absorbed at some wave lengths under some conditions was about thirty per cent.

The reaction conditions were such that usually the concentration of any product did not exceed two or three per cent. of that of the absorbing reactant. Thus the amount of reactants consumed was negligible, and reactions between products were minimized. On the other hand, products could be detected which were present in concentrations of 10^{-4} those of the reactants unless mass spectral cracking peaks of the reactants obscured the analysis. In some favorable cases products could be detected in concentrations of 10^{-5} those of the reactants.

The runs were performed either by scanning the complete spectrum (up to $m/e > 400$) during irradiation, or by monitoring one peak, or both. The former method gives more information, but the latter method gives higher accuracy. In either case background readings were observed before irradiation. In most of the runs where one peak was monitored, the decay curve of the peak in the dark was determined by discontinuing irradiation after the steady-state (in products) was achieved.

The mass spectra and sensitivity relative to oxygen were measured for each of C_2H_5I, CH_3CHO, C_2H_5OH, C_2H_5OOH, $C_2H_5OOC_2H_5$, CH_3OH, $CH_2\!-\!\underset{\diagdown\,\diagup}{O}\!-\!CH_2$, CO_2, and O_3. The mass spectra of I_2, H_2O and H_2O_2 were also observed, although quantitative data of peak heights could not be obtained because of adsorption in the metal lines. The calibration factor for C_2H_5OI was estimated by analogy with other compounds.

Five series of runs were made, at $25 \pm 2°$, with constant oxygen throughout, with variation of wave length, with variation of light intensity by means of a calibrated screen, and with variation of ethyl iodide pressure. For each series, qualitative studies were made by repeatedly scanning the complete spectrum up to m/e of 400 during irradiation. Quantitative curves of growth, initial rates, and steady-state pressures were found by monitoring a single mass peak, relative to O^{16}. The various products were analyzed in series, with some drift in the instrument and some variation in reproducing the initial chemical composition. At the completion of one cycle of the series, duplicate or triplicate runs were made. The final values of initial rates, half-lives, and steady-state pressure of products (relative to diffusion through the hole) are estimated to have a standard deviation of about 20 per cent. Though this error is disappointingly large, it must be remembered that the steady-state pressure of products was between 0.01 and 64 microns, or the order of magnitude of 0.01 to 100 millionths of an atmosphere.

Matheson tank oxygen was used, and impurities were 0.3 per cent. argon and 0.7 per cent. nitrogen. Eastman white label ethyl iodide was used. Impurity peaks were noted at m/e of 17 (H_2O), 18 (H_2O), and 59 in amounts of 11/30/5, respectively, relative to 10,000 for the parent peak at m/e of 156. The cracking pattern of ethyl iodide for 50 volt electron energy is given in Table I. Oxygen, of course, gives a heavy contribution to masses 16 and 32. The maximum yield of a given product in these studies was about one per cent. of the pressure of reactants, thus the mass numbers 14, 15, 25, 26, 27, 28, 29, 30 and 127 were unavailable for product analysis. Furthermore a small amount of a product $\pm$ 1 mass number of 127 could not be separated from the large I peak there. Thus these studies do not provide information on HI (128), C_2H_6 (30), C_2H_4 (28), HCHO (30), CO (28), CH_4 (16), C_2H_2 (26). Because of the background of water at mass numbers 17 and 18, the analysis of water is rather difficult.

TABLE I

MASS SPECTRUM OF ETHYL IODIDE RELATIVE TO PARENT PEAK HEIGHT OF 100 AT m/e = 156

m/e		Height	m/e		Height
12	C	0.63	28	C_2H_4	40.4
13	CH	1.65	29	C_2H_5	243.0
14	CH_2	5.73	30	$C^{13}C^{12}H_5$	6.1
15	CH_3	5.78	31	...	0.86
16	CH_4	...	59	...	0.05
17	OH	0.11	121	...	0.05
18	H_2O	0.30	127	I	50.0
24	C_2	1.28	141	CH_2I	2.33
25	C_2H	8.10	144	...	0.10
26	C_2H_2	70.2	148	...	0.69
27	C_2H_3	238.0	152	C_2HI	0.48
			156	C_2H_5I	100.0

Results

During irradiation product peaks were observed at m/e 17, 18, 19, 41–47, 62, 63.5, 90, 172 and 254. These peaks were identified as H_2O, CH_3CHO, C_2H_5OH, C_2H_5OOH, $C_2H_5OOC_2H_5$, C_2H_5OI, and I_2. (A minor peak around 286 was not identified.) The absolute pressures of $C_2H_5OOC_2H_5$, C_2H_5OOH, C_2H_5OH, and CH_3CHO could be determined from the calibrations of the respective compounds. In computing the CH_3CHO pressures it was assumed that the 42, 43, and 44 cracking peaks of C_2H_5OI were unimportant. This is almost certainly true, as the 45 peak could be satisfactorily accounted for from the other products. The 45 cracking peak of C_2H_5OI would certainly be much larger than the 42, 43, or 44 peaks. Of the four above-mentioned products the error in the C_2H_5OOH analysis is by far the greatest. For one thing C_2H_5OOH is a minor product. Of more importance however is the fact that the computation had to be made from the peak at m/e 62 which is mainly from $C_2H_5OOC_2H_5$.

I_2, C_2H_5OI, and H_2O could not be easily calibrated, but their pressures could be estimated. The calibration value used for iodine was adjusted to give a perfect carbon–iodine mass balance in the initial rates of series II of Table II. The sensitivity of C_2H_5OI was assumed to be similar to that for other iodine-containing compounds.

To within the calibration errors, no ethylene oxide or carbon dioxide were produced. C_2H_5OOI, CH_3COI, CH_3COOH, O_3, IO, IO_2, and H_2O_2 were not found. The first four compounds would have been easily detected if they were present in amounts exceeding 0.01 per cent. of ethyl iodide. The analysis of the latter three compounds is somewhat less sensitive because their masses are near mass spectral peaks of the reactants.

The experimental results are listed in Table II. For each of the six initial products (CH_3CHO, C_2H_5OH, I_2, $C_2H_5OOC_2H_5$, C_2H_5OI, C_2H_5OOH) and for each of the five series of runs there are listed; initial rates, R_i; the steady-state partial pressure, P_{ss}; the half-time of build up to this steady-state pressure with steady illumination, τ_L; the half-time of decay from the steady-state value after the light was turned off τ_D; and the steady state reaction rate, R_{ss}. The data P_{ss} and R_{ss} are also reported for water, which appeared

TABLE II

EXPERIMENTAL RESULTS IN TERMS OF: INITIAL RATES R_i, STEADY STATE PRESSURE P_{ss}; HALF-TIME TO REACH P_{ss} IN LIGHT, τ_L, HALF-TIME TO EMPTY CELL IN DARK, τ_D AND STEADY-STATE RATES, R_{ss}

Entry no.	Series no.		I	II	III	IV	V
1	O_2, mm.		2.8	2.8	2.8	2.8	2.8
2	C_2H_5I, mm.		2.8	2.8	2.8	0.20	0.055
3	λ_{min} Å.		2000	2200	2200	2200	2200
4	I_{abs}, photons/cc. sec. $\times 10^{-12}$		3.3	19.7	2.1	1.6	0.61
5	R_i 10^3 μ/sec.	CH_3CHO	36.5	225	23.1	20.6	10.2
6		EtOH	22.4	160	17.0	13.0	3.6
7		I_2	43.1	215[a]	29.1	13.4	6.5
8		$(EtO)_2$	1.8	12	1.7	1.0	
9		EtOI	16.2	94	12.0	4.0	0.48
10		EtOOH	12.4	43	5.5	4.2	2.4
11	P_{ss}, microns	CH_3CHO	10.8	60	8.8	7.6	2.0
12		EtOH	12.2	64	10.1	7.0	1.2
13		I_2	15.9	64	12.9	6.0	2.3
14		$(EtO)_2$	0.92	2.3	0.73	0.30	...
15		EtOI	2.6	7.4	2.2	0.22	0.03
16		EtOOH	0.11	1.2	...	0.11	...
17	τ_L, sec.	CH_3CHO	200	130	240	200	230
18		EtOH	280	200	300	300	300
19		I_2	323	210	300	260	315
20		$(EtO)_2$	225	105	230	160	...
21		EtOI	121	61	158	56	60
22		EtOOH	...	70	...	50	...
23	τ_D, sec.	CH_3CHO	...	...	...	235	...
24		EtOH	...	...	...	250	...
25		I_2	350	300	...	327	...
26		$(EtO)_2$	240	250	...	...	...
27		EtOI	...	90	123	38	30
28		EtOOH	...	...	...	...	...
29	R_{ss}, 10^3 μ/sec.	CH_3CHO	30	167	24	21	5.5
30		EtOH	34	177	28	19	3.3
31		I_2	33	134	27	13	4.8
32		$(EtO)_2$	2.5	6.4	2.0	0.8	
33		EtOI	5.5	16.0	4.7	0.47	0.07
34		EtOOH	0.3	3.0		0.3	0.0
35		H_2O	...		...	(7.8)	...

[a] Adjusted to give a carbon–iodine mass balance, see text.

with an induction period. The steady state is reached when the rate of formation of the product equals its rate of removal, both by chemical processes and effusion through the pinhole into the mass spectrometer. The intensity of absorbed light in Table II is computed assuming unit quantum yield for reaction a, and summation over the products. For the series IV, the detailed growth curves are presented in Figs. 2 and 3.

The results can be summarized in phenomenological terms, using the classifications of the appendix, with no reference to mechanism: (1) The initial measured products were C_2H_5OH, CH_3CHO, I_2, C_2H_5OOH, $C_2H_5OOC_2H_5$, and C_2H_5OI. Except for C_2H_5OI and possibly C_2H_5OOH, the initial rate of each product is directly proportional to absorbed light intensity. For the three series with constant C_2H_5I and O_2 but with intensity variation by means of screens, C_2H_5OI is also directly proportional to intensity; but for runs with varied C_2H_5I, the rate of formation of C_2H_5OI is roughly proportional to the product of absorbed intensity and concentration of C_2H_5I. That the products are formed at a rate proportional to rate of light absorption indicates (but does not fully prove) that none of these products were formed from radical-molecule reactions. The indication is that the products are produced directly or indirectly from radical-radical reactions. (2) Water is formed after an induction period, but it adsorbs and de-sorbs from the system in such a way that the results have very poor precision. (3) The curves of growth and steady-state values are such that the various products are examples of the following cases in terms of the Appendix: H_2O, Case 3; C_2H_5OOH, Case 5; C_2H_5OH, Case 4; C_2H_5OI, Case 2; CH_3CHO, I_2, and $(C_2H_5O)_2$ seem to be mild examples of Case 2 or Case 5, (later mechanistic considerations assign I_2 to Case 2 and the other two to Case 5). Thus at the steady-state condition, which corresponds to less than 7 per cent. reaction in all cases there are strong secondary reactions, and the situation differs considerably from that initially. (4) Alcohol, Case 4, is produced more rapidly at the steady-state than initially, whereas C_2H_5OI and C_2H_5OOH are destroyed.

Discussion

Initial Reaction.—The mechanism presented so far, reactions a, b, c, e, f and g for the initial rate,

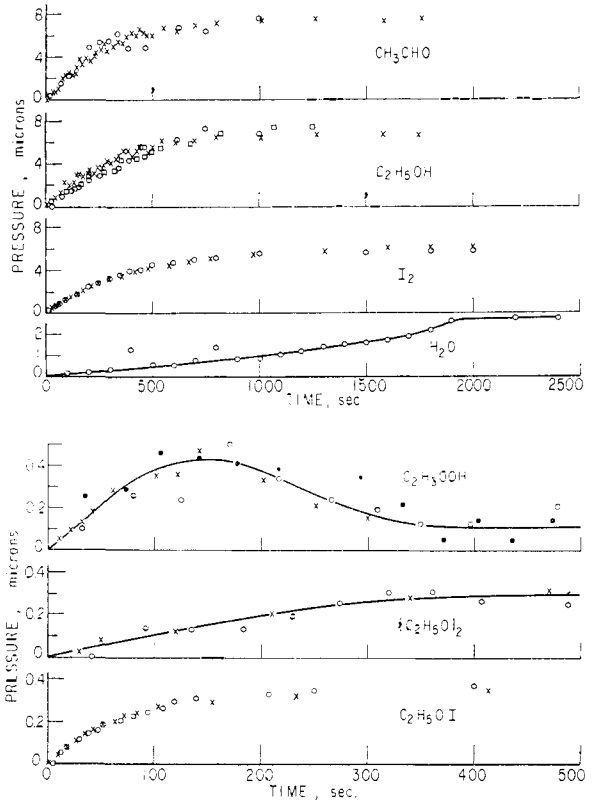

Fig. 2 (top) and 3.—Appearance of products as a function of time for series IV. Reactant pressures are given in Table II. The different symbols refer to duplicate runs.

predict all observed products except C_2H_5OOH and C_2H_5OI. Also, this mechanism, taken from the literature, predicts equal yields of CH_3CHO and C_2H_5OH. Entries 5 and 6 in Table II show that CH_3CHO is substantially higher than C_2H_5OH in all cases. Thus some process must compete with reaction f to produce CH_3CHO but not C_2H_5OH. A new process[16] analogous to reaction f that produces ethyl hydroperoxide and acetaldehyde seems to be indicated

$$CH_3CH_2OO + CH_3CH_2O \longrightarrow CH_3CH_2OOH + CH_3CHO \quad (h)$$

With this addition, the mechanism states that the sum of the rates of alcohol and hydroperoxide formation should equal the rate of aldehyde formation.

$$R_i(EtOH) + R_i(EtOOH) = R_i(CH_3CHO) \quad (1)$$

This relation is tested by entries 1 and 2 of Table III. It can be seen that aldehyde formation exceeds that predicted by the equation above. Thus a third source of formation of acetaldehyde is indicated, and the appearance of ethyl hypoiodite is not yet accounted for. A pair of reactions, bimolecular association or dismutation (compare steps f and g), fills both of the needs

$$I + CH_3CH_2O + M \longrightarrow CH_3CH_2OI + M \quad (i)$$

$$I + CH_3CH_2O \longrightarrow CH_3CHO + HI \quad (j)$$

These steps are added to the mechanism, and the initial rate of formation of hydrogen iodide is assumed to be the difference in entries 1 and 2 of Table III.

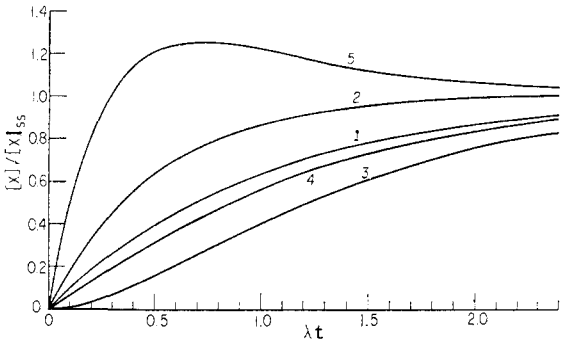

Fig. 4.—Development of product in stirred flow reactor: case 1, exponential build up of stable product after light turned on; case 2, same as Case 1 except product subject to first order chemical reaction; case 3, product is formed by secondary decay of another product; case 4, product formed directly from reactants and from secondary decay of another product; case 5, product formed directly from reactants but its formation is inhibited by another product.

An abbreviation is needed for the variable [M]. Russell and Simons[27] have shown that oxygen has only 0.026 the efficiency of ethyl iodide as a third body for reaction c. This relative efficiency is transferred to the other recombination of iodine atoms, reaction i. Thus one defines

$$[M] = [C_2H_5I] + 0.026\,[O_2] \quad (2)$$

and these values are listed in Table III.

In the further discussion it is assumed that the radicals reach their steady state very fast compared to the steady state of the products relative to diffusion through the pin-hole. Thus the steady-state analysis with respect to radicals can be applied to the initial rate data of the products. In the following section, the rate constant for reaction b, for example, will be written as k_b; but the rate of the reaction will be abbreviated by use of the symbol **b**, that is

$$\mathbf{b} = k_b[R][O_2][M] \quad (3)$$

In these terms the rates of formation of products are

$$\begin{array}{ll} R_i(EtOH) = \mathbf{f} & R_i(ETOI) = \mathbf{i} \\ R_i(Et_2O_2) = \mathbf{g} & R_i(HI) = \mathbf{j} \\ R_i(EtOOH) = \mathbf{h} & R_i(I_2) = \mathbf{c} \\ R_i(CH_3CHO) = \mathbf{f} + \mathbf{h} + \mathbf{j} & \end{array} \quad (4)$$

TABLE III

INTERPRETATION OF INITIAL RATE DATA

Entry	Series number	I	II	III	IV	V
1	$R_i(CH_3CHO)$, 10^3 μ/sec.	36.5	225.0	23.1	20.6	10.2
2	$R_i(EtOH) + R_i(EtOOH)$	34.8	203.0	22.5	17.2	6.0
3	$R_i(HI)$, calcd.	1.7	22.0	0.6	3.4	4.2
4	[M], eq. 3, mm.	2.9	2.9	2.9	0.27	0.13
5	$R_i(\Sigma I)/R_i(\Sigma C_2)$, eqs. 9, 10	1.14	1.0	1.17	0.78	1.02
6	$R_i(I_2)$	43.1	215.0	29.1	13.0	6.5
7	$R_i(EtOH) + R(EtOOH) + R(Et_2O_2)$	37.0	215.0	24.0	18.0	6.3
8	k_f/k_g, eq. 12	12.0	13.0	10.0	13.0	...
9	k_j/k_i, eq. 13, mm.	0.3	0.7	0.15	0.25	1.1
10	k_fk_e/k_i^2, eq. 14, mm.	10.2	10.8	9.5	3.0	14.3
11	k_fk_e/k_h^2, eq. 15a	6.7	21.8	18.5	11.0	4.8
12	k_fk_e/k_h^2, eq. 15b	5.0	19.5	14.0	14.0	4.5

(27) K. E. Russell and J. Simons, *Proc. Roy. Soc.* (*London*), **217A**, 271 (1953).

Making the steady-state assumption of zero net rate of formation of each radical, one finds

$$R_i(I) = 0 = a - 2c - i - j \quad (5)$$

$$R_i(EtOO) = 0 = a - b \quad (6)$$

$$R_i(EtOO) = 0 = b - 2e - h \quad (7)$$

$$R_i(EtO) = 0 = 2e - 2(f + g) - h - i - j \quad (8)$$

Combination of the above relations provides several consistency tests of the data and the mechanism. The total rate of light absorption is given by either of two expressions

$$I_{abs} = 2R_i(I_2) + R_i(EtOI) + R_i(HI) \quad (9)$$

$$I_{abs} = R_i(CH_3CHO) + R_i(EtOH) + 2R_i(Et_2O_2) + R_i(EtOOH) + R_i(EtOI) \quad (10)$$

Equation 9 is the sum of the rate of production of iodine containing products, R_i (ΣI), and eq. 10 is the sum of the rate of formation of ethyl containing products, R_i (ΣC_2). Entry no. 4 of Table II was computed from eq. 10. The ratio of eq. 9 to eq. 10 should be one, and it is given as entry 5 in Table III. The ratio scatters from 0.78 to 1.17 (the sensitivity of I_2 relative to O_2 was obtained by assuming this ratio to be unity for series II). This comparison illustrates the ± 20 per cent. error for reproducibility of data based on products present in relatively large amount.

Another consistency test from the mechanism is that

$$R_i(I_2) = R_i(EtOOH) + R_i(EtOH) + R_i(Et_2O_2) \quad (11)$$

This comparison is made as entries 6 and 7 of Table III, and in general this condition is met by the data.

The mechanism predicts the constancy of several ratios of constants. The division of products between reactions f and g should be constant, if reaction g is second order, not dependent on [M]. The ratio

$$R_i(EtOH)/R_i(Et_2O_2) = k_f/k_g \quad (12)$$

is entry 8 in Table III, and it varies only between 10 and 13 for the entire series with an average value of 12. This constancy indicates that f and g are, respectively, the only sources of ethanol and diethyl-peroxide, at initial times.

Similarly, the partitioning of HI and EtOI should be constant

$$R_i(HI)[M]/R_i(EtOI) = k_j/k_i \quad (13)$$

Equation 13 is tested by entry 9 in Table III, and the ratio is seen to scatter randomly over a range of a factor of 7 between extremes. This scatter does not lie in uncertainty as to [M] since series I, II, and III have identical values of initial reactant pressures. This scatter, in part, arises from the fact that $R(HI)$ was not observed directly but computed as the small difference in two large numbers, each subject to ± 20 per cent. error. The average value is 0.4 mm.

The mechanism further asserts that

$$\frac{R_i(EtOH)R_i(I_2)[M]}{\{R_i(EtOI)\}^2} = \frac{k_f k_c}{k_i^2} \quad (14)$$

This relation is tested as entry 10 in Table III. The first three series (with high reactant pressures) give good constancy for these ratios, but the last two series (with low ethyl iodide pressures) give scatter by a factor of 4. The average of all values is 9 mm.

Finally the mechanism predicts.

$$\frac{\{2R_i(I_2) + R_i(EtOI) + R_i(HI) - R_i(EtOOH)\}R_i(EtOH)}{2\{R_i(EtOOH)\}^2} = \frac{k_c k_f}{k_h^2} \quad (15a)$$

$$\text{and } \frac{\{I_a - R_i(EtOOH)\}R_i(EtOH)}{2\{R_i(EtOOH)\}^2} = \frac{k_c k_f}{k_h^2} \quad (15b)$$

Entries 11 and 12 of Table III indicate scatter over a range of a factor of 4 over the series. The average value of entry 12 is 12.

Subsequent Reactions.—As seen above, the error associated with the initial rate is large in this system, but the error and irreproducibility associated with the build-up to the steady-state is much greater. Very little quantitative information can be obtained from these data, the mechanism will be left incomplete, and one should merely look at the large quantitative trends in an effort to gain qualitative insight into the processes. As one inspects half-times to reach the steady state, steady-state pressures, or steady-state rates, one should not try to interpret the individual series, but rather pool the results of all five series in an effort to see the important effects.

The half-times to reach the steady-state, items 17–22 of Table II, can be compared with the normal value of about 250 seconds for all products except iodine and about 330 seconds for iodine for the diffusion constant through the hole. Acetaldehyde, iodine, and diethyl peroxide showed build-up times somewhat shorter than normal, indicating slight secondary attack or inhibition of these products as reaction proceeds. Ethyl hydroperoxide and ethyl hypoiodite show much shorter times than the diffusion time through the hole, indicating strong secondary destruction of these products. Ethyl hydroperoxide, in fact, goes through a pronounced maximum, and its steady-state pressure falls almost to zero, even though it is an important initial product. Ethyl alcohol shows a substantially longer time than normal, thus some secondary process forms alcohol. These data are summarized in Table IV.

The actual time evolution of the various products for series IV is given in Figs. 2 and 3. Qualitatively one notes that H_2O appeared after a pronounced induction period, and is presumably case 3 of the Appendix. Ethyl hydroperoxide goes through a well-defined maximum, and seems to be an example of case 5. Ethyl hypoiodite builds up to a steady-state more rapidly than other products, and seems to fit case 2.

At the steady state for *products*, the *net* rate of formation of any product R_{ss} is equal to the rate which the observed steady-state pressure of products leaks through the hole

$$R_{ss} = \lambda P_{ss} \quad (16)$$

These rates are listed as entries 29–35 in Table II. The total rate of photochemical formation of all products containing or derived from the ethyl group is

$$R_{ss}(\Sigma C_2) = R_{ss}(CH_3CHO) + R_{ss}(EtOH) + R_{ss}(EtOI) + R_{ss}(EtOOH) + 2R_{ss}(Et_2O_2) \quad (17)$$

TABLE IV

SUMMARY OF QUALITATIVE INFORMATION OBTAINED FROM DETAILED HALF-LIVES FOR ATTAINMENT OF STEADY-STATE FOR EACH PRODUCT

	CH_3CHO	EtOH	I_2	$(EtO)_2$	EtOI	EtOOH	H_2O
Initial rate							
Order with respect to light intensity	1	1	1	1	1	1	0
Subsequent processes							
Secondary production	No	Yes	No	No	No	No	Yes
Secondary inhibition or destruction	Slight	...	Slight	Slight	Strong	Strong	...
Effect of surfaces							
Adsorption noted	No	Some	Some	No	...	...	Serious
Decomposition noted	No	No	No	No	Probably	Yes	No

TABLE V

PARTIAL INTERPRETATION OF STEADY-STATE RATES

Entry	Series number	I	II	III	IV	V	Av.
1	$R_{ss}(\Sigma C_2)$, $10^3\ \mu$, eq. 17	77	376	61	42	(9.5)[a]	
2	$R_{ss}(\Sigma I)/R_{ss}(\Sigma C_2)$, eq. 19	0.93	0.76	0.96	0.68	(1.0)[a]	0.85
3	$R_i(\Sigma C_2)/R_{ss}(\Sigma C_2)$ $(R_{ss} - R_i)/R_{ss}(\Sigma C_2)$	1.19	1.45	1.00	1.03	(1.9)[a]	1.3
4	CH_3CHO	−0.06	−0.15	0.01	−0.01	−0.50	−0.25
5	EtOH	.15	.05	.18	.14	− .03	.10
6	$2Et_2O_2$	.02	.02	.01	− .01	(− .04)[a]	.0
7	EtOI	− .14	− .21	− .12	− .08	− .04	− .12
8	EtOOH	− .16	− .11	− .08	...	− .25	− .14
9	I_2	− .22	− .22	− .03	− .01	− .18	− .14
10	$10^5\ k_d/k_b$, moles/cc., eq. 22 $(R_{ss} - R_i')/R_{ss}(\Sigma C_2)$	.5	.3	...	...	.7	.5
11	CH_3CHO	− .01	.03	.01	.02	.0	− .01
12	EtOH	.20	.18	.18	.15	.25	.20
13	$2Et_2O_2$	.03	− .01	− .01	− .01	...	0
14	EtOI	− .11	− .13	− .12	− .08	− .02	−0.10
15	EtOOH	− .13	− .07	− .08	...	− .14	− .10

[a] Et_2O_2 not measured in series V. It was assumed to be $^1/_{12}$ EtOH.

and this quantity is entry no. 1 of Table V. The total rate of the photochemical reaction can be expressed in terms of iodine

$$R_{ss}(\Sigma I) = 2R_{ss}(I_2) + R_{ss}(EtOI) + R_{ss}(\text{other I}) \quad (18)$$

where R_{ss} (other I) includes the non-observable rate of formation of HI and the formation on the surface of purple non-volatile iodine-containing products (perhaps IO_2, solid). The total yield of observable iodine-containing compounds is

$$R_{ss}(\Sigma I) = 2R_{ss}(I_2) + R_{ss}(EtOI) \quad (19)$$

The ratio of observed iodide to observed ethyl' eqs. 19 and 17, is entry no. 2 of Table V. The ratio is seen to average 0.85 for the series; thus at least 15% of the iodide was lost in non-observable products under steady-state conditions. This loss (and the fact that some of it was a solid deposit on the surface) makes it impossible to carry out any further quantitative calculations on iodine at the steady state.

Initially the total rate for forming C_2-products, $R_i(\Sigma C_2)$, is found from a relation similar to eq. 17. The ratio of total rate of formation of C_2-compounds at initial times to the steady-state is given by entry 3 of Table V. On the average for all series, the total initial rate is about 30 per cent. faster than that at the steady state. It is interesting to compare initial rates with steady-state rates for each product, and this comparison (normalized by division by $R_{ss}(\Sigma C_2)$ for each series) is given by entries 4–9 in Table V. Ethyl alcohol is produced

TABLE VI

DESTRUCTION OF ETHYL HYPOIODITE IN THIS SYSTEM TIMES IN SECONDS FOR SERIES IV

Decay time in dark, τ_D	Previous irradiation time	Build up time in light, τ_L	Dark time preceding irradiation
76	382	56	∞
57	765	31	600
39	1684	34	300
38	2800	25	100

substantially faster at the steady-state than initially. For all other products, the net rate of production at the steady-state is slower than that for the initial reaction. The total decrease in CH_3CHO, EtOI, and EtOOH is substantially greater than the increase in rate of production of EtOH; and thus one has the experimental result that some one or more of these compounds is converted to ethanol.

Reaction d, well-established for methyl radicals, provides a natural explanation for secondary attack on iodine, and this possibility will be analyzed in a later paragraph. It is well-known in the literature that hydroperoxides react rapidly and heterogeneously on metal surfaces to produce aldehyde and water,[13] and this reaction was observed here when an effort was made to calibrate ethyl hydroperoxide in the mass spectrometer.

$$CH_3CH_2OOH \xrightarrow{\text{(surface)}} CH_3CHO + H_2O \quad (1)$$

Ethyl hypoiodite also was destroyed rapidly. The decay time in the dark was strongly dependent on the duration of the preceding irradiation, and the build-up in the light depended strongly on the duration of the preceding dark period, as can be seen in Table VI. The extra production of ethanol, the destruction of EtOI, and the accumulation of IO_2(?) on the surface is qualitatively accounted for by the steps

$$CH_3CH_2OI + H_2O\ (surf.) \longrightarrow C_2H_5OH + HOI\ (surf.) \quad (m)$$

$$CH_3CH_2O + HOI\ (surf.) \longrightarrow C_2H_5OH + OI\ (surf.) \quad (n)$$

$$CH_3CH_2O + HI \longrightarrow C_2H_5OH + I \quad (p)$$

Where (surf.) means "adsorbed on the surface." (The very minor product of mass number 286 might be a metastable oxide of iodine, I_2O_2.)

In terms of the 14 step mechanism written down above and in the notation of eq. 3, the steady-state rate of formation of products is

$$R_{ss}(CH_3CHO) = f + h + j + l$$

$$R_{ss}(EtOH) = f + 2m + p$$

$$R_{ss}(EtOI) = i - m$$

$$R_{ss}(Et_2O_2) = g$$

$$R_{ss}(EtOOH) = h - l$$

$$R_{ss}(I_2) = c - d$$

$$R_{ss}(HI) = j - p \approx 0$$

$$R_{ss}(IO_2, surf.) = n = m$$

$$R_{ss}(H_2O) = l - m$$

Making the steady-state assumption with respect to radical and atom formation and destruction, one finds

$$R(I) = a - 2c + d - i - j + p = 0$$

$$R(Et) = a - b - d = 0$$

$$R(EtOO) = b - 2e - h = 0$$

$$R(EtO) = 2e - 2(f + g) - h - i - j - n - p = 0$$

These equations lead to hopelessly complicated quadratic formulas when a general solution is attempted, except that the relation for ethyl radicals gives a simple result

$$[Et] = \frac{k_a(h\nu)[EtI]}{k_b[O_2][M] + k_d[I_2]} \quad (20)$$

With this equation, two general relations between initial rates R_i and steady-state rates can be derived

$$1 + \frac{k_d[I_2]_{ss}}{k_b[O_2][M]} = \frac{R_i(\Sigma I)}{R_{ss}(\Sigma I)} \quad (21)$$

$$= R_i(\Sigma C_2)/R_{ss}(\Sigma C_2) \quad (22)$$

Since HI and I (surface), presumably IO_2, were not observable in the mass spectrometer, only the second relation above can be used to estimate the ratio k_d/k_b, entry 10, Table V. The average value thus found for k_d/k_b for ethyl radicals is 0.5×10^{-5} mole/cc., and Christie's value[4] for the same quantity for methyl radicals is 18×10^{-5} mole/cc.

It proved impossible to get quantitative data on the rate of formation of water. Water continued to absorb on the surfaces and later de-gas over long periods of time. The consistency tests made for the initial rates by entries 6 and 7 of Table III cannot be extended to the steady-state rates because of the unavailability of data on the rate of water formation. Similarly the evaluation of rate constant ratios, as in entries 8–12 of Table III, cannot be carried out for the steady-state rate data.

It is of interest to compare the steady-state rate of each product with the initial rate reduced by the effect of inhibition by iodine, that is, the initial rate for each product is divided by the corresponding value of entry 3 in Table V. For each product these corrected rates R'_i are subtracted from the steady-state rate R_{ss} and normalized by $R_{ss}(\Sigma C_2)$. The quantities are entries 11–15 in Table V. This treatment corrects the initial rates for inhibition by iodine, step d, and compares the resulting rate with that observed at the steady state. This analysis indicates that diethyl peroxide, Et_2O_2 is a stable product in this system, in agreement with the mechanism above. Also acetaldehyde appears to be formed at the same *net* rate at the steady state as the initial rate corrected for iodine inhibition; however, the mechanism adds l to the rate. This is compensated for by the decrease in CH_3CHO production caused by reactions n and p. The mechanism correctly indicates that the increase in EtOH at the steady state should be about twice the decrease in EtOI.

Absence of Ozone.—Ozone is produced during the nitrogen dioxide sensitized photochemical oxidation of hydrocarbons in urban atmospheres, and it has been asked repeatedly whether reaction e', $RO_2 + O_2 \rightarrow RO + O_3$, could be a further contributor to the observed ozone. Ozone was calibrated in this mass spectrometer, and pressures as small 0.01 microns or about 10^{-8} atmospheres could have been detected. Ethyl iodide and the reaction products leave a clear mass "window" at $m/e = 48$. In this particular system ozone was absent, to these limits of detectability. Its absence might be due to its very high reactivity in this system, perhaps $O_3 + I \rightarrow O_2 + IO$: but it appears, from other studies already far advanced where no iodine is present, that ozone is absent because rate e is much faster than rate e' in this system. The rate of e' is favored by a high ratio of oxygen to free radical

$$R_e'/R_e = k_e'[O_2]/k_e[RO_2] \quad (23)$$

Series V was designed to favor this ratio so far as practicable, but again no ozone was observed.

It is concluded that ozone production by way of ethyl peroxy radicals and oxygen is an unimportant process.

Summary.—The present "stirred-flow" reactor with continual analysis of almost all products by the mass spectrometer does provide a sufficiently powerful method to give new insight into highly complicated reactions. By combining evidence from initial rates, steady-state pressures (at about 3% reaction), steady-state rates, build-up times, etc., as discussed in the Appendix, a great deal of information, independent of mechanism, was obtained. By combining these data with other studies in the literature, one confirms six elementary reactions from the literature a, b, c, d, e and f. From initial rate data with the identification of $(C_2H_5O)_2$, C_2H_5OOH, and CH_3CH_2OI, one is forced to postulate three additional steps

$$2CH_3CH_2O \longrightarrow CH_3CH_2OOCH_2CH_3 \quad (g)$$

$$CH_3CH_2OO + CH_3CH_2O \longrightarrow CH_3CH_2OOH + CH_3CHO \quad (h)$$

$$I + CH_3CH_2O + M \longrightarrow CH_3CH_2OI + M \quad (i)$$

(step h is similar to the process[16] in the methyl radical–oxygen system) and on less sure grounds one proposes a dismutation reaction in competition with reaction i

$$I + CH_3CH_2O \longrightarrow CH_3CHO + HI \quad (j)$$

Several secondary reactions were noted, the formation of ethanol and water and the destruction of CH_3CH_2OI and CH_3CH_2OOH, with strong implications that these are surface reactions. Five additional steps are tentatively proposed, although these are inadequate to explain all of the data.

In addition to the qualitative information obtained about products, some ratios of rate constants were obtained. The average values of these ratios of rate constants are summarized in Table VII. The fairly good reproducibility of k_f/k_g is taken to illustrate the precision of the instrument. The large scatter for the other ratios of rate "constants" is surely chemical in origin, rather than instrumental. That is, in spite of 9 steps for the initial rate and 14 elementary steps recognized for the entire process, some elementary step or steps is probably missing, or some product is formed in a manner other than assumed. Thus this study cannot claim quantitative completeness, but it does add new insight to the system.

TABLE VII

SUMMARY OF QUANTITATIVE INFORMATION OBTAINED FROM THESE STUDIES

Rate constant ratio	Units	Average value
k_f/k_g	.....	12 ± 2
k_i/k_i	Mole/cc.	$2 \pm 1.5 \times 10^{-8}$
$k_f k_e/k_i^2$	Mole/cc.	$5 \pm 3 \times 10^{-7}$
$k_f k_e/k_h^2$	.....	12 ± 6
k_d/k_b	Mole/cc.	$0.5 \pm 0.3 \times 10^{-8}$

Acknowledgment.—This work was supported by the Public Health Service, National Institute of Health, Project AP-104. The authors are deeply indebted to Dr. Richard J. Windgassen, Jr., who prepared the ethyl hydroperoxide and diethyl peroxide, and to Mr. Gardiner Myers who prepared the ozone. The authors also wish to thank Dr. Garnett McMillan and Professor Jack Calvert for useful discussions, and Dr. Fred Lossing for making available to us some of his mass spectral data.

Appendix

Interpretation of Curves of Growth.—In these highly complex systems it is proposed to classify each product on a phenomenological basis in terms of its buildup with time after the light is turned on and its decay with time as it leaks out of the pinhole after the light is turned off.

Products are formed by photochemical processes, and they disappear by leaking out the hole and by secondary chemical or photochemical reactions. Eventually a given product reaches a steady state where all the processes of its formation or destruction are balanced by the rate of leaking from the hole. The time behavior of a given product provides direct diagnostic information about its role in the reaction mechanism. The initial rate, the steady state concentration, and the mean-time to reach the steady state value give kinetic information and consistency tests. With this type of information available for a large number of products, one can make relatively complete statements about highly complex mechanisms. Different patterns of behavior shown by different modes of formation of products are developed below.

Case 0.—If the reaction cell is filled with reactants, connected to the large reservoir, and a small amount of substances of interest $[X]_0$ is added at time zero, the decay of X in the cell by transport out of the hole follows the differential equation

$$-d[X]/dt = \lambda[X] \quad (24)$$

and the integrated equation is

$$[X] = [X_0]e^{-\lambda t} \quad (25)$$

When $[X]/[X]_0$ is $1/e$, the time is defined as τ_0, so that

$$\lambda = 1/\tau_0 \quad (26)$$

The value of λ depends on cell volume and hole size. If the concentration of reactants is such that the mean free path is small compared to hole size, the flow will be jet or hydrodynamic flow; all substances X in the cell will be swept out at the same rate by the reactants.

If a product X is produced photochemically, its decay from the cell can be followed by turning off the light. If the product undergoes a dark reaction, the differential equation is

$$-d[X]/dt = \lambda[X] + k[X] \quad (27)$$

and the integrated equation is

$$[X] = [X_0]e^{-(k+\lambda)t} \quad (28)$$

When $[X]/[X]_0$ is $1/e$, the time is defined as τ; it is given by $1/(\lambda + k)$, and the value of k can be found from

$$(1/\tau) - (1/\tau_0) = k \quad (29)$$

On the other hand, if the product is formed by some persisting dark reaction, its differential equation after the light is cut off is

$$d[X]/dt = R - \lambda[X] \quad (30)$$

and the decay time is longer than τ_0. Similar behavior is shown if the substance X is seriously adsorbed on the surfaces of the cell and if it degasses during the dark period.

Case 1.—The reactants A, B, C, are held constant by connection to the large reservoir even though they leak out of the pinhole at a constant rate. At a convenient initial time the light of constant intensity I is turned on. One or more reactants absorb the light to give products. The initial rate R_x of production of X depends on concentration of reactants and light intensity, but these are constant. If the substance X does not undergo subsequent reaction nor is it produced by subsequent alternate reactions, its only mode of departure from the system is leakage through the hole. For this case the differential and integral equations are

$$d[X]/dt = R(x) - \lambda[X] \quad (31)$$

$$\lambda[X] = R(x)(1 - e^{-\lambda t}) \quad (32)$$

For early times, expansion of eq. 32 gives

$$[X]_i = R(x)t \quad (33)$$

so that the rate of production of X, $R(x)$, can be measured as the limit of $[X]/t$ as t approaches zero. As time approaches infinity, the product assumes a steady-state value

$$[X]_{ss} = R(x)/\lambda \quad (34)$$

When the product is within $1/e$ of its final value, that is, when $[X]/[X]_{ss} = 1 - 1/e$, the time is defined as τ_1, and it can be seen that

$$\tau_1 = 1/\lambda \quad (35)$$

Consistency tests to see whether the mechanism is really as simple as assumed here are

$$R(x)\tau_1 = [X]_{ss} \quad (36)$$

$$\tau_1 = \tau_0 \quad (37)$$

In Fig. 4 the full curve, eq. 32, in dimensionless form, $[X]/[X]_{ss}$ is plotted against λt. In later discussions, other curves are compared against Case 1 as a standard of reference.

Case 2.—This case is exactly like Case 1 except it is assumed that the product X is consumed at a rate that is

first order in X, although the first order rate constant k could depend on any of the variables held constant; reactants, light intensity, etc. The differential and integral equations are

$$\frac{d[X]}{dt} = R(x) - (k + \lambda)[X] = R(x) - \lambda_x[X] \quad (38)$$

$$\lambda_x[X] = R(x)(1 - e^{-\lambda_x t}) \quad (39)$$

where $\lambda_x = k + \lambda$. For short times, expansion of eq. 39 shows that the initial rate is

$$[X]_i = R(x)t \quad (40)$$

exactly as for Case 1. As time approaches infinity the steady state is unlike Case 1

$$[X]_{ss} = R(x)/(\lambda + k) \quad (41)$$

When $[X]/[X]_{ss}$ has attained the value of $1 - 1/e$, the time is defined as τ_2, and from eq. 39 this is seen to be

$$1/\tau_2 = \lambda_x = k + \lambda \quad (42)$$

Consistency tests for this mechanism are that

$$R(x)\tau_2 = [X]_{ss} \quad (43)$$

$$\tau_2 < \tau_0 \quad (44)$$

The present case gives additional information in that the difference of $1/\tau_2$ and $1/\tau_0$ is the rate constant for secondary chemical or photochemical reaction of the product X

$$\frac{1}{\tau_2} - \frac{1}{\tau_0} = k \quad (45)$$

By varying initial reactant concentrations or light intensity, one finds the order of the initial rate $R(x)$ and the secondary decay rate k with respect to these variables. A comparison of Case 1 and Case 2, each with the same initial rate, is given in Fig. 4 for the special case of $k = \lambda$.

If this constant is the same as that found for decay from the cell during a dark interval (eq. 29), the two rates are identified as being between the substance X and a relatively stable molecular species, or the substance X decomposes on the wall or undergoes a unimolecular decomposition. If the rate constant from eq. 45 is greater than that found from eq. 29, it indicates that the reaction of X for Case 2 is with a free radical.

Case 3.—A case of especial interest is that a product X is not formed directly from the reactants A, B, C, etc., but it is formed from an intermediate Q that itself is produced directly from reactants. The mechanism for this case is

$$A + bB + \cdots \xrightarrow{R_Q} qQ + \cdots \xrightarrow{k_Q} xX + \cdots \quad (46)$$

The differential equation for Q is

$$d[Q]/dt = R(Q) - (\lambda + k_Q)[Q] = R(Q) - \lambda_Q[Q] \quad (47)$$

which is identical to eq. 38, that is, Q is an example of Case 2. The differential equation for X is

$$d[X]/dt = k_Q[Q] - \lambda_x[X] \quad (48)$$

The integrated equation for Q is of the form of eq. 39 and the integrated equation for the product of interest is

$$[X] = \frac{R(Q)k_Q}{\lambda_Q}\left[\frac{1}{\lambda_x} + \frac{e^{-\lambda_Q t}}{(\lambda_Q - \lambda_x)} - \frac{\lambda_Q}{\lambda_x(\lambda_Q - \lambda_x)} e^{-\lambda_x t}\right] \quad (49)$$

Expansion of (49) gives

$$[X] = R(Q)k_Q\left[\frac{t^2}{2} - (\lambda_Q + \lambda_x)\frac{t^3}{6} + \cdots\right] \quad (50)$$

Equation (50) has no linear terms in t and thus X builds up after an induction period. For $t < 0.3/(\lambda_Q+\lambda_x)$, all terms higher than second order in t can be omitted and the resulting error will be less than ten per cent. As time approaches infinity, both Q and X reach steady state values

$$[Q]_{ss} = R(Q)/\lambda_Q \quad (51)$$

$$[X]_{ss} = [Q]_{ss}k_Q/\lambda_x \quad (52)$$

Thus one can obtain the rate constant k_Q from the ratio of steady-state concentrations. If the induction period τ_{in} is defined as the time for X to reach two per cent. of its steady-state value, then

$$1/\tau_{in} = 5(\lambda_x\lambda_Q)^{1/2} \quad (53)$$

If k_Q is very large compared to λ_x, Q reaches its steady-state value much sooner than does X, and for times long compared to $1/\lambda_Q$ the expression for X becomes

$$\lambda_x[X] = R(Q)(1 - e^{-\lambda_x t}), \text{ if } k_Q >> \lambda \quad (54)$$

Thus for this special situation, Case 3 reduces to Case 2. This situation is routinely encountered where Q is an active free radical intermediate, and X is the product of the free radical process. The induction period is too short to be detected.

Case 3 is illustrated in Fig. 4 for a special case where both k_Q and λ_x are assumed to be equal to the constant λ.

Case 4.—One product X may be produced directly from reactants, another Y may be formed by a parallel process, and Y may react to produce additional amounts of X. The differential equations are

$$d[Y] = R(y) - \lambda_y[Y] \quad (55)$$

$$d[X]/dt = R(x) + k_y[Y] - \lambda_x[X] \quad (56)$$

where $\lambda_y = \lambda + k_y$ and $\lambda_x = \lambda + k_x$. The integrated equation for Y is that for Case 2, and the integrated equation for X is

$$[X] = \frac{R(x)}{\lambda_x}\left[1 + \frac{R(y)}{R(x)}\frac{k_y}{k_y - k_x}\right](1 - e^{-\lambda_x t}) - \frac{k_y}{k_y - k_x}\frac{R(y)}{\lambda_y}(1 - e^{-\lambda_y t}) \quad (57)$$

The initial reaction is given by

$$[X]_i = R(x)t \quad (58)$$

The steady state is

$$[X]_{ss} = \frac{R(x)}{\lambda_x} + \frac{R(y)k_y}{\lambda_y\lambda_x} = \frac{R(x)}{\lambda_x} + [Y]_{ss}\frac{k_y}{\lambda_x} \quad (59)$$

This case has the same initial rate as Case 1, but builds up to a higher steady-state value. After normalization to the same steady-state value, this case is plotted in Fig. 4, where it is assumed that $k_y = \lambda$, $k_x = 0$, and $R(x) = R(y)$.

If a large number of products are followed as a function of time, one may deduce which products Y are attacked to produce extra amounts of some product X by the following test. The term λ_x can be measured from the curve of growth of X. The constant k_y can be measured from the curve of growth of Y and eq. 45. The steady-state rate of production of X, $R_{ss}'(X)$, is $\lambda_x[X]_{ss}$. Thus from eq. 59 and 45 one finds

$$R'_{ss}(X) - R_i(X) = k_y[Y]_{ss} = \left(\frac{1}{\tau_y} - \frac{1}{\tau_0}\right)[Y]_{ss} \quad (60)$$

If the same values of k_y are found by each method above, it is good evidence that the radical attacking Y produces X or that Y is converted to X.

Case 5.—One product X is produced from reactants and undergoes further reaction as in Case 2, another product Y is formed from reactants and Y inhibits the further formation of X. The inhibition may take the form of $R(X)/(1 + \alpha[Y])$ which simplifies to $R(x) - k_y[Y]$ if $\alpha[Y] << 1$. The approximate form is much easier to integrate, and will be selected as this example. The differential equations are

$$d[Y]/dt = R(y) - \lambda_y[Y] \quad (61)$$

$$d[X]/dt = (R(x) - k_y[Y]) - \lambda_x[X] \quad (62)$$

The integrated equation for Y is that for Case 2, and the integrated equation for X is

$$[X] = \frac{R(x)}{\lambda_x}\left[1 - \frac{R(y)}{R(x)}\frac{k_y}{k_y - k_x}\right][1 - e^{-\lambda_x t}] + \frac{k_y}{k_y - k_x}\frac{R(y)}{\lambda_y}[1 - e^{-\lambda_y t}] \quad (63)$$

The initial rate is

$$[X]_i = R_x t \quad (64)$$

The steady state is

$$[X_{ss}] = \frac{R(x)}{\lambda_x} - \frac{R(y)}{\lambda_y}\frac{k_y}{\lambda_x} = \frac{R(x)}{\lambda_x} - [Y_{ss}]\frac{k_y}{\lambda_x} \quad (65)$$

However, if $\lambda_x > \lambda_y$ (that is, $k_x > k_y$), then X goes through a maximum value before reaching the steady state. A sample curve is given in Fig. 4 where it is assumed that $k_y = \lambda$, $k_x = 2\lambda$, and $R(x) = R(y)$. The pronounced maximum is diagnostic of a strong degree of inhibition by other products.